Shabanpour, Javad; Simovski, Constantin

On the design of reflecting intelligent surfaces for multi-user NOMA communication networks

Published in:
ISCAS 2024 - IEEE International Symposium on Circuits and Systems

DOI:
10.1109/ISCAS58744.2024.10558543

Published: 01/01/2024

Document Version
Peer-reviewed accepted author manuscript, also known as Final accepted manuscript or Post-print

On the design of reflecting intelligent surfaces for multi-user NOMA communication networks

Javad Shabanpour*, Constantin Simovski,
Department of Electronics and Nanoengineering, School of Electrical Engineering, Aalto University,
P.O. Box 15500, FI-00076 Aalto, Finland,
mohammadjavad.shabanpoursheshpoli@aalto.fi*

***Abstract*—Reconfigurable intelligent surfaces offer potential opportunity for wireless signal manipulation. In Power Domain Non-Orthogonal Multiple Access (P-D NOMA), ensuring users receive specific power from the base station is vital. Our paper introduces a semi-analytical method using unequal coefficients superposition to derive closed-form formulas for estimating the beam directivity in large RISs. Employing simplifications to achieve these formulas, we validate their accuracy via full-wave simulations.**

***Index Terms*—RIS, PD-NOMA, 6G, Metasurface**

I. Introduction

Demand for faster wireless networks drives research in high-frequency communication (e.g., millimeter-wave, terahertz) for 5G and 6G [1], [2]. Despite wider bandwidth, it is limited by shorter communication range and signal loss [3]. Reconfigurable Intelligent Surfaces (RISs) with active/passive elements reshape environments, enhancing wireless links, signal quality, coverage, and power efficiency [4], [5]. By Incorporating tunable and switchable electronic devices into the metasurface [6]–[8], the manipulation of the wireless environment can be programmed in a real time.

In scenarios involving multiple users or receivers, it is crucial to effectively receive electromagnetic waves from the base/broadcasting station. A weakly directive radiation pattern capable to transmit the signal to all users disperses energy which is mostly wasted. Another approach is time division multiplexing (TDM) that involves a single-beam RIS which redirects the beam to users versus time. However, meeting the stringent latency demands of 5G and 6G networks, which require ultra-fast (few microseconds) switching between users, TDM becomes not optimal. The third solution involves Space Division Multiplexing, that implies M beams for M users. It cam be achieved partitioning the RIS into M sections each of them serves a single beam reflector. However, this straightforward approach reduces the overall surface directivity, and to uphold Quality of Service, a significant increasing of the RIS size is necessary that indeed restricts its efficiency and applicability in urban conditions. Instead, one may make the RIS of given dimensions multi-periodic so that it would generate N beams [9].

Power Domain Non-Orthogonal Multiple Access (PD-NOMA) approach revolutionizes wireless network efficiency by allocating power levels, departing from traditional orthogonal multiple access where each user gets a distinct resource block [10]. PD-NOMA enables multiple users to share time and frequency resources, allotting lower power levels to stronger channel users and higher levels to weaker ones. Its benefits include fairness, enhanced spectral efficiency, and low latency compared to conventional methods [11]. Currently, the sole approach for allotting predetermined power in multi-beam RIS is optimization-based techniques, a process that is time-consuming and falls short of meeting the low-latency demands of higher-frequency wireless communication.

In our paper, we use the known phased-array method for engineering the multi-beam RIS for PD-NOMA networks. We use the local-reflection approximation to ensure that each unit cell scatters the incoming wave without impacting the adjacent unit cell. In this approximation, the multiple-beam RIS is a superposition of M generic single-beam RISs, whose reflection phase profiles superimpose [9]. This method allows one to control the angles of M scattered waves, but the control of their amplitudes (i.e. individual power adjustment for each user) is difficult. Meanwhile, the RIS-based PD-NOMA network demands the predetermined power intensity scattering pattern of the RIS. To resolve this issue we propose a new analytical method resulting for a large but finite-size metasurface-based RIS in closed-form formulas allowing one to estimate the directivity of every emitted beam. Although some simplifying hypotheses are used, we show that these formulas are accurate enough and promise to drastically simplify the design of a multi-beam RIS for PD-NOMA networks.

II. Background and Theoretical Framework

Previously, efforts have been done on quantifying antenna array directivity, with endeavors to streamline its calculation for linear and planar arrays [12], [13]. Multi-beam antenna arrays find broad application in communication and surveillance systems like MIMO, electronic countermeasures, direct broadcasting, and multiple-target radar systems [14]. Extensive research has tackled the development of asymmetric multi-beam reflect-arrays, capable of generating multiple reflected beams with varying gain levels [15], [16]. Nayeri et al. [17] introduced an optimization-based technique for realizing a single-feed reflect-array, which, however, comes with a high computational overhead.

In [9], a comprehensive method for achieving multi-receiver RIS using the superposition principle has been outlined. The equation for multi-beam formation is Eq. (3) of [9]. Let

us show that by incorporating M real-valued multiplicative constants, denoted as a_i, within the conventional superposition process, it becomes viable to control the absolute directivity of each emitted beam. We use a weighted combination of individual phase-only local reflection patterns:

$$a_1 e^{j\phi_1} + a_2 e^{j\phi_2} + ... + a_M e^{j\phi_M} = |b|\, e^{j\phi_T} \tag{1}$$

In the above equation, $e^{j\phi_T}$ and b both depending on the coordinates represent the local reflection phase and amplitude of a resulting multi-periodic metasurface (MS). We assume that $e^{j\phi_i}, i \in [1...M]$, represent the generic MSs with uniform excitation and gradient phase distribution, i.e. ϕ_i linearly depends on the Cartesian coordinates ($\phi_i = \xi_i^x x + \xi_i^y y$). Since the MSs have deeply subwabelength unit cells, we neglect the specular reflection and assume that each generic MS produces a single beam pointing at (θ_i, φ_i) direction.

The far-field radiation/scattering pattern of any finite flat surface is the 2D Fourier transform of the complex-amplitude excitation pattern (see e.g. in [18]). Indeed, the Fourier transform of $e^{j(\xi_i^x x + \xi_i^y y)}$ over the infinite plane xy is a delta-function. However, on this stage we take into account the finite sizes L_x, L_y of the MS and deal with its realistic scattered pattern. In the 2D case ($L_y \to \infty$, $\xi_{1,2}^y = 0$) we evidently have

$$F_i(\theta) = \frac{jk}{2} \int\limits_{-L_x/2}^{L_x/2} e^{-jkx(\sin\theta - \sin\theta_i)} dx = \operatorname{sinc}\frac{kL_x}{2}(\sin\theta - \sin\theta_i), \tag{2}$$

where $\sin\theta_i \equiv \xi_i^x/k$ and $\operatorname{sinc} u \equiv \sin u/u$. The generalization of Eq. (2) to the 3D case will be done below. Notice that the angular functions $F_i(\theta, \varphi)$ in the theory of radiating aperture are referred as aperture directivity factors. Since our effective aperture is a homogenized phased array we will call these functions phased array directivity factors.

Eq. 1 in terms of its Fourier transform (denoted F) can be written in a form:

$$a_1 F_1(\theta, \varphi) + a_2 F_2(\theta, \varphi) + ... = F_T(\theta, \varphi) \tag{3}$$

Eventually, the peak of the multi-beam MS in the i-th direction can be calculated as follows:

$$D(\theta_i, \varphi_i) = \frac{4\pi F_T(\theta_i, \varphi_i) F_T^*(\theta_i, \varphi_i)}{\int_0^{2\pi} \int_0^{\pi/2} F_T(\theta, \varphi) F_T^*(\theta, \varphi) \sin\theta d\theta d\varphi} \tag{4}$$

For simplicity and without sacrificing generality, we present the further analysis for two scattered beams directed at (θ_1, φ_1) and (θ_2, φ_2). Our initial approximation is as follows. We neglect the side-lobe levels in the structure and postulate that $F_2(\theta_1, \varphi_1) \simeq 0$, and $F_1(\theta_2, \varphi_2) \simeq 0$. In accordance to [15], [19], this approximation is reasonable for large MSs ($L \gg \lambda$). In this approximation, partial beams are mutually orthogonal:

$$\int\limits_0^{2\pi} \int\limits_0^{\pi/2} F_1(\theta, \varphi) F_2^*(\theta, \varphi) \sin\theta d\theta d\varphi \simeq 0 \tag{5}$$

We employ Eq. 5 as a mean to achieve closed-form expressions. Though this assumption subjects to certain constraints, it holds with minimal deviations for realistic RISs. For both peak values of directivity Eq. (4) together with Eq. (5) gives

$$D(\theta_{1,2}, \varphi_{1,2}) = \frac{4\pi a_{1,2}^2 |F_{1,2}(\theta_{1,2}, \varphi_{1,2})|^2}{\sum\limits_{i=1}^{2} \int\limits_0^{2\pi} \int\limits_0^{\pi/2} a_i^2 |F_i(\theta, \varphi)|^2 \sin\theta d\theta d\varphi} \tag{6}$$

For the power flux density P_{rad} in both peak directions we easily obtain

$$P_{rad}(\theta_i) \approx P_b / \cos\theta_i, \tag{7}$$

where P_b is the flux density in the broadside direction.

To calculate the integrals in the denominator of the expression (6) we use the variable exchange

$$\psi_x = kL(\sin\theta\cos\varphi - \sin\theta_0\cos\varphi_0),$$

$$\psi_y = kL(\sin\theta\sin\varphi - \sin\theta_0\sin\varphi_0)$$

that imply

$$d\psi_x d\psi_y = (kL)^2 \sin\theta\cos\theta d\theta d\varphi \tag{8}$$

Here $k = 2\pi/\lambda$ is the wave number, $L = L_x = L_y$ is the size of the MS, and (θ_0, φ_0) are angles (θ_1, φ_1) for the first integral ($i = 1$ in Eq. (6)) and angles (θ_2, φ_2) for the second integral ($i = 2$ in Eq. (6)).

For the peak values of directivity we then obtain

$$D(\theta_{1,2}, \varphi_{1,2}) \cong \frac{4\pi k^2 L^2 a_{1,2}^2 |F'(0,0)|^2}{\left(\frac{a_1^2}{\cos\theta_1} + \frac{a_2^2}{\cos\theta_2}\right)\left(\int\int_\Omega |F'(\psi_x, \psi_y)|^2 d\psi_x d\psi_y\right)}, \; \Omega = (\psi_x)^2 + (\psi_y)^2 \le k^2 L^2 \tag{9}$$

Prime in $F'(\psi_x, \psi_y)$ denotes the phased array directivity factor F_T after the variable change. In the numerator this factor is taken in the broadside direction because both $\theta = \theta_{1,2}$ together with $\varphi = \varphi_{1,2}$ correspond to $\psi_x = \psi_y = 0$ for F', uniting both partial beams. Assuming that the incidence plane is either xy or yz we may present the directivity factor of a planar array as a product of two linear directivity factors (see e.g. in [20]). In our notations, it can be written as follows:

$F'(\psi_x, \psi_y) \cong F'(\psi_x) \cdot F'(\psi_y)$. It allows us to easily integrate F' (integral of $\mathrm{sinc}u$ in the limits $[-\pi, \pi]$ is tabulated) and rewrite Eq. (9) in a following form:

$$D(\theta_{1,2}, \varphi_{1,2}) \cong \frac{\pi a_{1,2}^2}{\left(\frac{a_1^2}{\cos\theta_1} + \frac{a_2^2}{\cos\theta_2}\right)} D_x D_y = \frac{\pi a_{1,2}^2}{\left(\frac{a_1^2}{\cos\theta_1} + \frac{a_2^2}{\cos\theta_2}\right)} \times \frac{2L}{\lambda} \times \frac{2L}{\lambda} = \frac{a_{1,2}^2}{\left(\frac{a_1^2}{\cos\theta_1} + \frac{a_2^2}{\cos\theta_2}\right)} \times \frac{4\pi L^2}{\lambda^2} \quad (10)$$

In the above equations, D_x denotes the maximal directivity of a uniform linear array stretched along x in the xz plane, and D_y denotes the same maximum in the yz plane for the array along y. In our case, the array length L along x and y is the same, and $D_x = D_y = 2L/\lambda$ [21]. Therefore, Eq. (10) separately written for two scattering maxima takes form:

$$D(\theta_1, \varphi_1) = \frac{\cos\theta_1}{1 + \left(\frac{a_2}{a_1}\right)^2 \left(\frac{\cos\theta_1}{\cos\theta_2}\right)} \times D_{\max}, \quad (11)$$

$$D(\theta_2, \varphi_2) = \frac{\left(\frac{a_2}{a_1}\right)^2 \cos\theta_1}{1 + \left(\frac{a_2}{a_1}\right)^2 \left(\frac{\cos\theta_1}{\cos\theta_2}\right)} \times D_{\max}. \quad (12)$$

Here $D_{\max} = 4\pi L^2/\lambda^2$ is maximal directivity of the square aperture [21]. Our final formulas for a two-beam reflecting MS follow from these equations and take form:

$$\frac{D(\theta_2, \varphi_2)}{a_2^2} = \frac{D(\theta_1, \varphi_1)}{a_1^2}, \quad (13)$$

$$\left(\frac{D(\theta_1, \varphi_1)}{\cos\theta_1} + \frac{D(\theta_2, \varphi_2)}{\cos\theta_2}\right) = D_{\max}. \quad (14)$$

The generalization of (13) and (14) to the case $M > 2$ is straightforward:

$$\frac{D(\theta_i, \varphi_i)}{a_i^2} = \mathrm{const(i)}, \quad (15)$$

$$\sum_{i=1}^{M} \frac{D(\theta_i, \varphi_i)}{\cos\theta_i} = D_{\max}. \quad (16)$$

These equations allow one to find the constants a_i which offer the needed scattering patter. Once we know these numbers, we find the amplitude $b(x, y)$ and phase $\phi_T(x, y)$ distribution of the local reflection coefficient. Then within the assumption of the reflection locality we may discretize our homogeneous MS with a mesh $N \times N$ of small unit cells and design the unit cells which offer the needed complex reflection coefficients at the mesh points. This task is beyond the scope of the present paper.

The solution of Eqs. (15) and (16) leaves arbitrary for a_1. Therefore, we put $a_1 = 1$, find other a_i and finally perform the normalization of the amplitude b so that $b(x, y) \leq 1$.

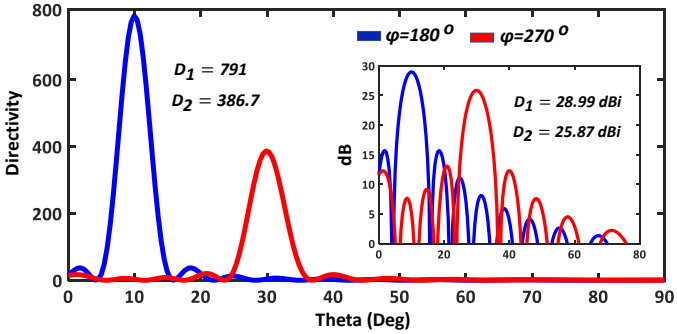

Fig 1. Directivity intensity pattern (in both linear and decibel formats) for asymmetrically oriented two-beams RIS with scattering maxima at $(10°, 180°)$ and $(30°, 270°)$.

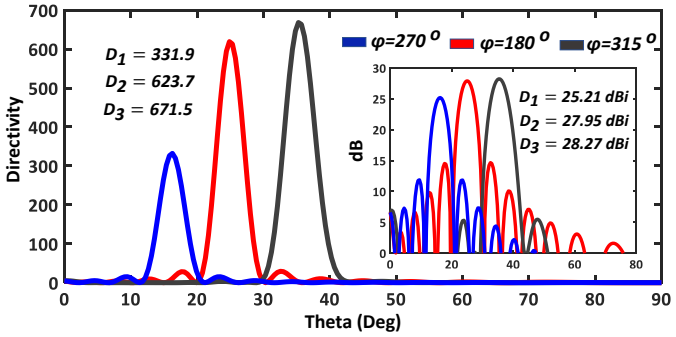

Fig 2. Directivity intensity pattern (linear and decibel) for a RIS with three asymmetrically oriented beams pointing at desired angles $(16.3°, 270°)$, $(25°, 180°)$, and $(35.3°, 315°)$) with $D_1 = 25.23$, $D_2 = 28$, and $D_3 = 28.3$ dBi.

Indeed, our approach implies some power loss in the MS. The limits of validity of our approach need to be checked via more accurate simulations. First, the partial beams orthogonality, and therefore Eqs. (15) and (16) lose validity when $\theta_i \to 90°$ because the beams for large scattering angles are wide. Also, the key assumption $L \gg \lambda$ may restrict the angles of scattering maxima for which the method is applicable. Indeed, our approximate method needs a verification.

Concept Verification

In order to exactly calculate the scattering pattern we use the integral formula from [9] combining the Huygens principle with antenna array theory. It implies an impenetrable boundary illuminated by a plane wave with given reflection amplitude and phase distributions. We have built a MATLAB code calculating the scattering pattern in this way. In our numerical examples, the RIS dimension is $L = 10\lambda$, that implies $D_{\max} =$ 31dBi.

In the first example, we study the two-beam RIS: Here the RIS dimension is $L = 10\lambda$, that implies $D_{\max} = 31$dBi, the angles of maximal scattering are $(\theta_1, \varphi_1) = (10°, 180°)$ and $(\theta_2, \varphi_2) = (30°, 270°)$) with prescribed directivity of $D_1 =$ 29 dBi in the $(10°, 180°)$ direction. Due to a fixed maximum directivity, the directivity in the second direction is calculated using Eq. 14 that gives $D_2 = 25.9$ dBi. Applying Eq. 14

Table 1. Comparison between the exact (E_1) and approximate (E_2) value of total scattered power (not normalized to the incident power).

$$E_1(\times 10^4) = \int_0^{2\pi}\int_0^{\pi/2} |F_1(\theta,\varphi) + F_2(\theta,\varphi)|^2 \sin\theta d\theta d\varphi \qquad E_2(\times 10^4) = \int_0^{2\pi}\int_0^{\pi/2} |F_1(\theta,\varphi)|^2 + |F_2(\theta,\varphi)|^2 \sin\theta d\theta d\varphi$$

N	L	1 $\theta_1 = 10^o, \varphi_1 = 180^o$ $\theta_2 = 30^o, \varphi_2 = 270^o$			2 $\theta_1 = 20^o, \varphi_1 = 180^o$ $\theta_2 = 50^o, \varphi_2 = 270^o$			3 $\theta_1 = 10^o, \varphi_1 = 180^o$ $\theta_2 = 30^o, \varphi_2 = 180^o$		
		E1	E2	Error(%)	E1	E2	Error(%)	E1	E2	Error(%)
30	10λ	1.7801	1.7807	0.03	2.1469	2.1440	0.1	1.8354	1.7897	3
24	8λ	1.1434	1.1423	0.1	1.3781	1.377	0.1	1.0616	1.1423	7
15	5λ	0.4561	0.4505	1.3	0.535	0.533	0.3	0.397	0.4505	13

we obtain $a_1 = 1$ and $a_2 = 0.7$. Ultimately, we apply these constants to Eq. 1. As a result, the input energy is redirected into two asymmetric beams with predetermined directivity values: $D_1 = 28.99$ and $D_2 = 25.87$ dBi. Fig. 1 depicts the absolute directivity of the emitting beams that effectively aligns with the target values and desired tilt angles. We see that for angles of scattering maxima not exceeding 30° our method works very well.

In the second example, we assess a three-beam RIS with desired tilt angles at $(16.3^\circ, 270^\circ)$, $(25^\circ, 180^\circ)$, and $(35.3^\circ, 315^\circ)$. Target absolute directivities are $D_1 = 25.23$, $D_2 = 28$, and $D_3 = 28.3$ dBi. Utilizing Eq.14, the RIS requires a superimposed phase-amplitude pattern with ($a_1 = 1$, $a_2 = 1.425$, $a_3 = 1.38$) so that to generate three beams with predetermined directivities (see Fig. 2). The RIS, driven by the proper phase-amplitude pattern from Eq. 1, produces beams with maximal directivity values ($D_1 = 25.21$, $D_2 = 27.95$, $D_3 = 28.27$ dBi) close to theoretical predictions, with errors under 1%. So, for angles of scattering maxima not exceeding 35° the method works well also for three-beam RISs.

In Table 1 we present the values of total radiated (scattered) power by the MS denoted E. For simplicity it is not normalized to that of the incident wave flux impinging on the MS and therefore can be higher than unity. In this table, nine numerical examples of a two-beam RIS are presented (with 3 different scattering maxima and 3 different sizes of the MS). In accordance to the definition presented in the Table $(E1, E2)$ respectively denote E calculated rigorously and in the approximation of the partial beams orthogonality. We see that our approximate method remains valid even for a RIS with a quite modest size $L = 5\lambda$ and even for a scattering maximum corresponds to a substantial polar angle 50°. However, if the azimuthal angles of two scattered beams are the same, the accuracy of our method worsens (Example 3, $L = 5\lambda$). Indeed, it is the consequence of the non-exact orthogonality of two partial beams whose tails in this case slightly intersect.

III. Conclusion

We have demonstrated that an additive combination of distinct constant-amplitude gradient-phase excitations enables engineering a multi-beam RIS using quite simple closed-formulas that allows one to avoid extensive full-wave simulations on the RIS design stage. As a proof of concept, we offer illustrative examples showcasing accurate prediction of predetermined directivities for multi-beam RISs at desired angles. By adhering to certain constraints, our approach facilitates designing such RISs without lengthy optimization, that is important for P-D NOMA communication advancement.

Acknowledgment

This project has received funding from the European Union's Horizon 2020 research and innovation program under the Marie Skłodowska-Curie grant agreement No 956256.

References

[1] M. A. ElMossallamy, H. Zhang, L. Song, K. G. Seddik, Z. Han, and G. Y. Li, "Reconfigurable intelligent surfaces for wireless communications: Principles, challenges, and opportunities," *IEEE Transactions on Cognitive Communications and Networking*, vol. 6, no. 3, pp. 990–1002, 2020.

[2] M. Di Renzo, A. Zappone, M. Debbah, M.-S. Alouini, C. Yuen, J. De Rosny, and S. Tretyakov, "Smart radio environments empowered by reconfigurable intelligent surfaces: How it works, state of research, and the road ahead," *IEEE journal on selected areas in communications*, vol. 38, no. 11, pp. 2450–2525, 2020.

[3] T. S. Rappaport, Y. Xing, O. Kanhere, S. Ju, A. Madanayake, S. Mandal, A. Alkhateeb, and G. C. Trichopoulos, "Wireless communications and applications above 100 ghz: Opportunities and challenges for 6g and beyond," *IEEE access*, vol. 7, pp. 78729–78757, 2019.

[4] Q. Wu and R. Zhang, "Intelligent reflecting surface enhanced wireless network via joint active and passive beamforming," *IEEE Transactions on Wireless Communications*, vol. 18, no. 11, pp. 5394–5409, 2019.

[5] Z. Ji, P. L. Yeoh, D. Zhang, G. Chen, Y. Zhang, Z. He, H. Yin, *et al.*, "Secret key generation for intelligent reflecting surface assisted wireless communication networks," *IEEE Transactions on Vehicular Technology*, vol. 70, no. 1, pp. 1030–1034, 2020.

[6] J. Shabanpour, "Programmable anisotropic digital metasurface for independent manipulation of dual-polarized thz waves based on a voltage-controlled phase transition of vo 2 microwires," *Journal of Materials Chemistry C*, vol. 8, no. 21, pp. 7189–7199, 2020.

[7] J. Shabanpour and C. R. Simovski, "Angular and polarization stability of broadband reconfigurable intelligent surfaces of binary type," *IEEE Access*, vol. 10, pp. 126253–126268, 2022.

[8] J. Shabanpour, V. Lenets, G. Lerosey, S. Tretyakov, and C. Simovski, "Engineering of intelligent reflecting surfaces: Reflection locality and angular stability," *arXiv preprint arXiv:2308.10589*, 2023.

[9] H. Taghvaee, A. Jain, S. Abadal, G. Gradoni, E. Alarcón, and A. Cabellos-Aparicio, "On the enabling of multi-receiver communications with reconfigurable intelligent surfaces," *IEEE transactions on nanotechnology*, vol. 21, pp. 413–423, 2022.

[10] T. Hou, Y. Liu, Z. Song, X. Sun, Y. Chen, and L. Hanzo, "Reconfigurable intelligent surface aided noma networks," *IEEE Journal on Selected Areas in Communications*, vol. 38, no. 11, pp. 2575–2588, 2020.

[11] Y. Liu, X. Mu, X. Liu, M. Di Renzo, Z. Ding, and R. Schober, "Reconfigurable intelligent surface-aided multi-user networks: Interplay between noma and ris," *IEEE Wireless Communications*, vol. 29, no. 2, pp. 169–176, 2022.

[12] H. Bach, "Directivity of basic linear arrays," *IEEE Transactions on Antennas and Propagation*, vol. 18, no. 1, pp. 107–110, 1970.

[13] A. H. Nuttall and B. A. Cray, "Approximations to directivity for linear, planar, and volumetric apertures and arrays," *IEEE journal of oceanic engineering*, vol. 26, no. 3, pp. 383–398, 2001.

[14] K. Kagoshima, S. Takeda, and K. Itou, "Array excitation coefficients of a compact multi-beam antenna for mimo applications," in *2014 IEEE-APS Topical Conference on Antennas and Propagation in Wireless Communications (APWC)*, pp. 195–198, IEEE, 2014.

[15] H. Rajabalipanah, A. Abdolali, J. Shabanpour, A. Momeni, and A. Cheldavi, "Asymmetric spatial power dividers using phase–amplitude metasurfaces driven by huygens principle," *ACS omega*, vol. 4, no. 10, pp. 14340–14352, 2019.

[16] P. Nayeri, F. Yang, and A. Z. Elsherbeni, "Design and experiment of a single-feed quad-beam reflectarray antenna," *IEEE transactions on antennas and propagation*, vol. 60, no. 2, pp. 1166–1171, 2011.

[17] P. Nayeri, F. Yang, and A. Z. Elsherbeni, "Design of single-feed reflectarray antennas with asymmetric multiple beams using the particle swarm optimization method," *IEEE Transactions on Antennas and Propagation*, vol. 61, no. 9, pp. 4598–4605, 2013.

[18] S. Liu, T. J. Cui, L. Zhang, Q. Xu, Q. Wang, X. Wan, J. Q. Gu, W. X. Tang, M. Qing Qi, J. G. Han, *et al.*, "Convolution operations on coding metasurface to reach flexible and continuous controls of terahertz beams," *Advanced science*, vol. 3, no. 10, p. 1600156, 2016.

[19] L. Bao and T. J. Cui, "Tunable, reconfigurable, and programmable metamaterials," *Microwave and Optical Technology Letters*, vol. 62, no. 1, pp. 9–32, 2020.

[20] M. Khalaj-Amirhosseini, "Synthesis of concurrent multibeam and conical beam antenna arrays," *International Journal of RF and Microwave Computer-Aided Engineering*, vol. 29, no. 12, p. e21966, 2019.

[21] C. A. Balanis, *Antenna theory: analysis and design*. John wiley & sons, 2016.